TiO2 microspheres containing magnetic nanoparticles for intra-arterial hyperthermia

著者	Kanetaka Hiroyasu, Liu Gengci, Li Zhixia, Miyazaki Toshiki, Furuya Maiko, Kudo Tada-aki, Kaw Masakazu
journal or publication title	Journal of Biomedical Materials Research Part B: Applied Biomaterials
volume	105
number	8
page range	2308-2314
year	2016-08-06
URL	http://hdl.handle.net/10228/00006941

doi: info:doi/10.1002/jbm.b.33765

TiO_2 microspheres containing magnetic nanoparticles for intra-arterial hyperthermia

Hiroyasu Kanetaka[1], Gengci Liu[2], Zhixia Li[3], Toshiki Miyazaki[4], Maiko Furuya[1], Tada-aki Kudo[1], Masakazu Kawashita[2]

[1]Graduate School of Dentistry, Tohoku University, Sendai 980-8575, Japan

[2]Graduate School of Biomedical Engineering, Tohoku University, Sendai 980-8579, Japan

[3]School of Chemistry and Chemical Engineering, Guangxi University, Nanning 530004, China

[4]Graduate School of Life Science and Systems Engineering, Kyushu Institute of Technology, Kitakyushu 808-0196, Japan

Correspondence to: M. Kawashita; E-mail: m-kawa@ecei.tohoku.ac.jp

Running head: TiO_2 microspheres for intra-arterial hyperthermia

Abstract: Magnetic microspheres measuring 15–35 μm in diameter are believed to be useful for intra-arterial hyperthermia. In the present study, we attempted to prepare titanium dioxide (TiO_2) microspheres containing magnetic nanoparticles (MNPs). MNP-containing TiO_2 microspheres with diameters of approximately 30 μm were successfully obtained by sol-gel reaction of titanium tetraisopropoxide in a water-in-oil emulsion with added cosurfactant of 1-butanol and subsequent heat treatment at 200°C. The microspheres showed ferrimagnetism owing to high content of MNPs in approximately 60 wt% and had a low-crystalline TiO_2 matrix. Furthermore, the agar phantom was heated to above 43°C after approximately 1 min under an alternating magnetic field of 100 kHz and 300 Oe and showed *in vitro* biocompatibility similar to that of MNP-free TiO_2 microspheres.

Keywords: magnetic nanoparticles; TiO_2; microspheres; hyperthermia

INTRODUCTION

Hyperthermia is a minimally invasive treatment for malignant tumors that has minor side effects. In clinical practice, the tumor is heated externally by utilizing hot water, microwave heating, ultrasonic heating, or other methods. However, these conventional heating methods are not effective for tumors that occur in deeper regions of the body. Recently, local hyperthermia treatment using magnetic materials has received considerable attention, because magnetic materials can generate heat by relaxation loss or hysteresis loss under an alternating magnetic field of 100–300 kHz.[1,2] Moreover, clinical trials examining the efficacy of thermotherapy using magnetic nanoparticles have been attempted in the United States of America (USA) and in countries in the European Union (EU).[3-5]

Local hyperthermia using magnetic nanoparticles, as described above, may be a promising next-generation tumor treatment. Similarly, research in our laboratory has focused on intra-arterial hyperthermia using magnetic microspheres measuring 15–35 μm in diameter.[6-10] To date, ferrimagnetic magnetite microspheres,[6] magnetic nanoparticle (MNP)-containing silica (SiO_2) microspheres,[7] iron-containing SiO_2 microspheres[8], and MNP-containing titanium dioxide (TiO_2) microspheres[9,10] have been prepared, and their structures, magnetic properties, and *in vitro* heat-generating ability have been investigated. However, MNP-containing TiO_2 microspheres have a mean diameter smaller than 10 μm, which is too small for intra-arterial therapy.

In our previous study, we used the sol-gel reaction of titanium alkoxide in water-in-oil (W/O) emulsion during preparation of the MNP-TiO_2 microspheres. It is difficult to increase the sizes of the microspheres only by modification of reaction conditions because hydrolysis and polycondensation reactions of titanium alkoxide can occur easily. On the other hand, in a micro-emulsion reaction system, addition of cosurfactant, such as a short-chain alcohol, can affect the shapes and sizes of the micro-emulsion droplets,[11,12] and similar effects can be expected in our W/O emulsion reaction system.

Accordingly, in this study, we aimed to obtain larger microspheres by adding 1-butanol as a cosurfactant to the reaction system. We then investigated the structures, magnetic properties, *in vitro* heat-generating ability, and *in vitro* biocompatibility of the resulting microspheres.

MATERIALS AND METHODS

Sol-gel synthesis of samples

The oil phase consisted of 40 g of kerosene, 3 g of sorbitan monooleate (span 80), 1 g of sorbitan monostearate (span 60), and 3 mL of 1-butanol. The oil phase was then placed in a water bath and heated to 30°C for 20 min while being stirred with a homogenizer at approximately 1,500 rpm. Here, in order to obtain homogeneity of the oil phase, the surfactants of span 60 and span 80 were first added to kerosene, and 1-butanol was then added to the mixture of surfactants and kerosene. Commercially available MNPs (product no.

637106; Sigma-Aldrich Corp., USA) of 3 g were then introduced into the oil phase along with 4.2 mL of ultrapure water while being vigorously stirred.

The water phase, which consisted of 2.7 g methanol, 4.5 g titanium tetraisopropoxide (TTIP), and 3.2 g diethanolamine, was added to the stirred solution. In this study, we prepared samples with different total reaction times of 30 min (10 min at 30°C, 10 min at 40°C, and 10 min at 55°C) or 60 min (20 min at 30°C, 20 min at 40°C, and 20 min at 55°C). Samples prepared with total reaction times of 30 and 60 min were denoted as samples RT-30 and RT-60, respectively. The gel particles were separated by centrifugation at 1,735 × *g* for 5 min and washed with ethanol four times. The gel particles were then dried at 36.5°C for 12 h and 150°C for 3 h. In order to prevent oxidization of MNPs, heat treatment was applied at 200°C for 3 h. As a reference sample for *in vitro* biocompatibility tests, MNP-free TiO_2 microspheres were also prepared. Unless indicated, all reagents used were obtained from Wako Pure Chemical Industries (Japan).

Characterization of samples

The crystalline phase of the samples was verified by powder X-ray diffraction (XRD; Miniflex 600HDA; Rigaku, Japan) using the following settings: X-ray source, CuKα; X-ray power, 40 kV, 15 mA; scanning rate, $2\theta = 10°$/min. Particle sizes and crystal morphologies of the samples were observed with a scanning electron microscope (SEM; VE-8800; Keyence,

Japan) and particle size distribution analyzer (Microtrac HRA [9320-X100]; Nikkiso, Japan).

Measurement of the magnetic properties of samples

The saturation magnetization (*Ms*) and coercive force (*Hc*) of the samples were measured with a vibrating sample magnetometer (VSM; VSM-5; Toei, Japan) in magnetic fields up to 10 kOe at room temperature at a frequency of 80 Hz. We assumed that the area of the hysteresis loop measured under the applied magnetic field (100 kHz, 300 Oe) was the same as that measured in a field of 300 Oe using the VSM. The heat generated by the samples was calculated using the following equation:[13]

$$P = f \oint HdB \times 10^{-7}$$

where f is frequency (in Hz), H is the magnetic field strength (in Oe), and B is the magnetization (in emu) of a sample in an applied magnetic field. The term $\oint HdB$ is the area of the hysteresis loop in the applied magnetic field. Therefore, in our calculations, f = 100 kHz and the area of the hysteresis loop measured at 300 Oe using the VSM was substituted for $\oint HdB$.

Measurement of the *in vitro* heat-generating ability of samples

A mass of 0.2 g of a sample was dispersed into a 3-mL hot agar solution (agar content = 1.0 wt%) in a glass tube, and the agar was then solidified in cold water. The concentration of the

sample in the agar phantom was 67 mg/mL. The glass tubes containing the samples were placed in an applied alternating current magnetic field of 100 kHz and 300 Oe, in accordance with our previous studies.[14] The heat generated by the samples was investigated by measuring changes in the temperature of the agar phantom as a function of time using a fiber optic temperature sensor (TempSens; Opsens Inc., Canada).

Evaluation of the *in vitro* biocompatibility of samples

Similar to our previous study,[9] the *in vitro* biocompatibility of samples was evaluated using fibroblasts. Rat-derived Rat-1 fibroblasts were cultured in Dulbecco's modified Eagle's medium (DMEM; Wako Pure Chemical Industries, Japan) containing 10% horse serum (Thermo Fisher Scientific, Waltham, MA, USA), 100 U/mL penicillin (Meiji Seika Kaisha, Ltd., Japan), and 100 μg/mL streptomycin (Meiji Seika Kaisha, Ltd., Japan). The cells were routinely subcultured every third day in a 60.1-cm^2 culture dish at 37°C in humidified air with 5% CO_2.

Cell experiments were conducted by establishing the following three groups: a control group (untreated); a TiO_2 group (MNP-free TiO_2 microspheres); and an MNP-containing TiO_2 group (RT-30 and RT-60). A cell suspension consisting of 1×10^4 Rat-1 fibroblasts was seeded in each well of a 24-well plate with 0.8 mL medium. Using 24-well cell culture inserts, which have a porous membrane bottom with a 1.0-μm pore size (Corning, Tewksbury, MA,

USA), test samples (TiO_2, RT-30, and RT-60) were added to the wells by deposition on the membranes of the inserts. The sample groups (TiO_2, RT-30, and RT-60) were tested at a concentration of 1.2 mg/well. Cell proliferation was examined after 1, 3, and 7 days of culture. Total DNA from the cells was extracted using an AllPrep DNA/RNA/Protein Mini Kit (Qiagen GmbH, Germany) in accordance with the manufacturer's protocol.[15] Following extraction, the DNA concentrations were measured by absorbance at 260 nm using a spectrophotometer (GeneQuant Pro, GE Healthcare, UK).[16] The values are given as mean DNA content, and were derived from five replicates per sample. The results are expressed as means ± standard deviations.

Statistical analysis

Differences between groups were analyzed using Student's *t*-tests. Differences with *P* values of less than 0.05 were considered significant.

RESULTS AND DISCUSSION

Figure 1 shows the XRD patterns of samples RT-30 and RT-60 in comparison with that of starting MNPs. Sharp diffraction peaks ascribed to magnetite (Fe_3O_4; PDF: 19-0629) and/or maghemite (γ-Fe_2O_3; PDF: 39-1346) were observed for the present samples and starting MNPs, and no diffraction patterns for crystalline TiO_2 were observed. In this study, the heat

treatment of samples was carried out at 200°C to avoid unwanted oxidation of starting MNPs into antiferromagnetic hematite. At the heat treatment temperature of 200°C, the crystallinity of TiO_2 matrix was still low; therefore, the samples used in this study did not yield obvious XRD peaks for crystalline TiO_2. These results indicate that the present samples contained MNPs and had a low-crystalline TiO_2 matrix.

Figure 2 shows SEM images of samples RT-30 and RT-60. Spherical microspheres of approximately 20–30 μm in diameter were successfully obtained. There was no significant difference in the morphology of microspheres between samples RT-30 and RT-60, indicating that the difference in reaction time barely affected the morphology of the resulting sample. Figure 3 shows size distribution curves for samples RT-30 and RT-60. The present samples yielded a size distribution in the range from 20 to 40 μm, with one vertex at 30 μm. Notably, the size distribution of sample RT-60 was slightly broader than that of RT-30. Although the specific mechanism underlying this effect is unclear, the longer reaction time may cause growth and deterioration of microspheres simultaneously. In fact, the broader size distribution of sample RT-60 could also be observed in lower-magnification SEM images (Fig. 2).

The sizes of microspheres are critical for intra-arterial hyperthermia. Microspheres should have diameters similar to those of capillary vessels (approximately 15–35 μm) in order to allow them to embolize the capillary vessels surrounding the tumors. The results shown in Figs. 2 and 3 suggested that the samples used in the present study almost met the

requirements of embolic agents, and illustrated that the addition of 1-butanol as a cosurfactant was effective for increasing the sizes of microspheres from a few micrometers to several dozen micrometers. The increase in the sizes of microspheres by addition of a cosurfactant can be interpreted as follows. Without cosurfactant, the elasticity and tenacity of the surfactant layer around the emulsion droplet may be low. The crystal nucleus can agglomerate to form microspheres in the droplet as hydrolysis and polycondensation of TTIP progress, and the mass of microspheres increases as the sizes of the microspheres increase. When the sizes of microspheres have increased up to several micrometers, the interfacial surfactant layer around the emulsion droplet is broken because of the mass of the microspheres, resulting in demulsification. As a result, small microspheres are formed without cosurfactant. In contrast, with a cosurfactant such as 1-butanol, the fluidity of the interfacial surfactant layer can be greatly increased; thus, the interfacial tension of oil-water interfaces can decrease, whereas the elasticity and tenacity of the surfactant layer can increase.[17] Accordingly, the formed interfacial surfactant layer allows microspheres to increase to the upper bounds of the diameter and mass of microspheres and therefore, the resulting microspheres are many times larger than those prepared without cosurfactant.

Table 1 shows *Ms*, *Hc*, and calculated MNP contents of samples in comparison with those of starting MNPs. The *Ms* was determined by magnetization curves under an applied magnetic field of 10 kOe. The *Ms* values of samples RT-30 and RT-60 were 42.8 and 44.3

emu/g, respectively; these values were lower than that of the starting MNPs (73.2 emu/g). There are two possible explanations for the lower *Ms* values of samples compared with that of starting MNPs. First, the content of MNPs in samples was lower than that of starting MNPs. Second, the coating layer on the MNPs may weaken the superexchange interaction between the magnetic moments on iron ions and induce a spin disorder on the surface of MNPs, resulting in a lower *Ms* compared with that of starting MNPs.[18,19]

The *Hc* values of samples RT-30 and RT-60 were 45.0 and 100.0 Oe, respectively. The TiO_2 shell encapsulating the MNP screens and decreases the magnetic dipole coupling interactions between neighboring MNPs, thereby reducing the *Hc* measured from hysteresis loops of samples. On the other hand, Fe_3O_4 in the starting MNPs may be partially converted to γ-Fe_2O_3 in samples during the sol-gel synthesis procedure. The particle size of γ-Fe_2O_3 converted from Fe_3O_4 is likely to be much larger than that of Fe_3O_4.[20] For single-domain magnetic particles, the *Hc* increases as the size of the particles increases.[21] This factor could lead to the observed increase in the *Hc* values of the samples. For sample RT-60, the *Hc* was almost same as that of the starting MNPs (98.0 Oe) because the two opposite effects described above may be well balanced. However, for sample RT-30, Fe_3O_4 in starting MNPs may be only partly converted to γ-Fe_2O_3 since the sol-gel synthesis procedure reaction time is relatively short. As a result, the effects of the TiO_2 shell may be dominant, resulting in a significant reduction in *Hc* for sample RT-30.

To avoid evaluation errors and to obtain accurate absolute heating measurements, the specific absorption rate (*SAR*) of each sample was analyzed by measuring *in vitro* heat-generation of samples. Figure 4 shows the time-dependent temperature curves of the agar phantom under a magnetic field of 100 kHz and 300 Oe. Both of the present samples heated the agar phantom to above 43°C after approximately 1 min. From the increase in temperature, the value of *SAR* was calculated using the following equation:[20]

$$SAR = \frac{\sum_i C_i m_i}{m_{sample}} \frac{\Delta T}{\Delta t}$$

where m_{sample} is the mass of sample and $C_i m_i$ is the heat capacity of each component whose temperature is increased in the applied magnetic field (C_{agar} = 4.2 J/g/K, $C_{magnetite}$ = 0.62 J/g/K, and $C_{titania}$ = 0.69 J/g/K)[22]. The term $\Delta T/\Delta t$ is the largest gradient of the time-dependent temperature curve. The *SAR* values calculated for sample RT-30, sample RT-60, and starting MNPs are listed in Table 2. Figure 5 shows the magnetization curves of samples measured under an applied magnetic field of 300 Oe. The heat generated (*P*) by samples was calculated from the area of these curves and is listed in Table 2.

We speculates that hysteresis loss mainly contributed to the heat generation of sample RT-60 because the *SAR* value (20 W/g) was lower than the heat generation *P* (22.3 W/g) calculated from the area of the hysteresis loop.[10] On the other hand, the *SAR* value of sample RT-30 (19.2 W/g) was higher than the heat generation *P* (9.1 W/g), suggesting that relaxation loss rather than hysteresis loss may contribute to the heat generation of sample RT-30. As

described above, the TiO_2 shell encapsulating the MNPs may screen and decrease the magnetic dipole coupling interactions between neighboring MNPs for sample RT-30, which decreases *Hc* and *P* calculated from the hysteresis loop.

Figure 6 shows the DNA concentrations of Rat-1 fibroblasts cultured with different samples. No significant differences in DNA concentrations were observed between each group after 1 day; however, there were significant differences in DNA concentrations between the control group and the TiO_2 and sample groups after 3 and 7 days. Because of the low heat temperature of 200°C used in this study, it was possible that some chemical reagents remained in microspheres and were released into the cell culture medium. Generally, higher temperatures are favorable for improving the chemical durability of microspheres; however, the heat treatment at high temperatures may oxidize MNPs into antiferromagnetic hematite. Additionally, heat treatment at higher temperatures with controlled oxygen partial pressure may be effective in improving the *in vitro* biocompatibility of microspheres. On the other hand, we found that there were no significant differences in DNA concentrations between the TiO_2 and sample groups, suggesting that incorporation of MNPs into TiO_2 microspheres did not adversely affect the *in vitro* biocompatibility of microspheres. In addition, Rat-1 fibroblasts grown in medium with TiO_2, sample RT-30, or sample RT-60 did not show significant morphological damage after 1, 3, or 7 days of culture (Figure 7). Their morphologies remained similar to that of the control group.

CONCLUSION

TiO_2 microspheres containing MNPs of approximately 30 μm in diameter were successfully obtained by addition of a cosurfactant into a W/O emulsion reaction system. The TiO_2 microspheres containing MNPs (Fe_3O_4 and/or γ-Fe_2O_3) of approximately 60 wt% increased the temperature of the agar phantom to above 43°C after 1 min and showed *in vitro* biocompatibility similar to that of MNP-free TiO_2 microspheres. The TiO_2 microspheres containing MNPs investigated in the present study are expected to be useful for intra-arterial hyperthermia-based treatment of cancer. However, the biocompatibility of these microspheres should be further improved by heat treatment at higher temperatures, and additional *in vivo* biocompatibility assessments should be performed.

ACKNOWLEDGMENTS

This work was supported by a research grant from the Magnetic Health Science Foundation, Japan. The authors thank to Prof. Masahiro Hiraoka, Kyoto University, for his cooperation in measurement of the heat-generating ability of samples.

REFERENCES

1. Jordan A, Scholz R, Maier-Hauff K, Johannsen M, Wust P, Nadobny J, Schirra H,

Schmidt H, Deger S, Loening S, Lanksch W, Felix R. Presentation of a new magnetic field therapy system for the treatment of human solid tumors with magnetic fluid hyperthermia. J Magn Magn Mater 2001;225:118–126.

2. Li Z, Kawashita M, Araki N, Mitsumori M, Hiraoka M, Doi M. Magnetite nanoparticles with high heating efficiencies for application in the hyperthermia of cancer. Mater Sci Eng C 2010;30:990–996.
3. Johannsen M, Gneveckow U, Eckelt L, Feussner A, Waldofner N, Scholz R, Deger S, Wust P, Loening SA, Jordan A. Clinical hyperthermia of prostate cancer using magnetic nanoparticles: presentation of a new interstitial technique. Int J Hypertherm 2005;21:637–647.
4. Thiesen B, Jordan A. Clinical applications of magnetic nanoparticles for hyperthermia. Int J Hyperthermia 2008;24:467–474.
5. van Landeghem FK, Maier-Hauff K, Jordan A, Hoffmann KT, Gneveckow U, Scholz R, Thiesen B, Bruck W, von Deimling A. Post-mortem studies in glioblastoma patients treated with thermotherapy using magnetic nanoparticles. Biomaterials 2009;30:52–57.
6. Kawashita M, Tanaka M, Kokubo T, Inoue Y, Yao T, Hamada S, Shinjo T. Preparation of ferrimagnetic magnetite microspheres for *in situ* hyperthermic treatment of cancer. Biomaterials 2005;26:2231–2238.
7. Li Z, Kawashita M, Araki N, Mitsumori M, Hiraoka M, Doi M. Magnetic SiO_2 gel

microspheres for arterial embolization hyperthermia. Biomed Mater 2010;5:065010.

8. Li Z, Kawashita M, Doi M. Sol-gel synthesis and characterization of magnetic TiO_2 microspheres. J Ceram Soc Japan 2010;118:467–473.
9. Li Z, Kawashita M, Kudo T, Kanetaka H. Sol-gel synthesis, characterization and *in vitro* compatibility evaluation of iron nanoparticle encapsulating-silica microspheres for hyperthermia of cancer. J Mater Sci Mater Med 2012;23:2461–2469.
10. Liu G, Kawashita M, Li Z, Miyazaki T, Kanetaka H. Sol-gel synthesis of magnetic TiO_2 microspheres and characterization of their *in vitro* heating ability for hyperthermia treatment of cancer. J Sol-Gel Sci Tech 2015;75:90–97.
11. di Meglio JM, Dvolaitzky M, Taupin C. Determination of the rigidity constant of the amphiphilic film in “birefringent microemulsions”; the role of the cosurfactant. J Phys Chem 1985;89:871–874.
12. Farago B, Richter D, Huang JS, Safran SA, Milner ST. Shape and size fluctuations of microemulsion droplets: the role of cosurfactant. Phys Rev Lett 1990;65:3348–3351.
13. Luderer AA, Borrelli NF, Panzarino JN, Mansfield GR, Hess DM, Brown JL, Hahn EW. Glass-ceramic-mediated, magnetic-field-induced localized hyperthermia: response of a murine mammary carcinoma. Rad Res 1983;94:190–198.
14. Kawashita M, Domi S, Saito Y, Aoki M, Ebisawa Y, Kokubo T, Saito T, Takano M, Araki N, Hiraoka M. *In vitro* heat generation of ferrimagnetic maghemite microspheres for

hyperthermic treatment of cancer under alternating magnetic field. J Mater Sci Mater Med 2008;19:1897–1903.

15. Xu C, Houck JR, Fan W, Wang P, Chen Y, Upton M, Futran ND, Schwartz SM, Zhao LP, Chen C, Mendez E. Simultaneous isolation of DNA and RNA from the same cell population obtained by laser capture microdissection for genome and transcriptome profiling. J Mol Diagn 2008;10:129–134.
16. Shutoh Y, Takeda M, Ohtsuka R, Haishima A, Yamaguchi S, Fujie H, Komatsu Y, Maita K, Harada T. Low dose effects of dichlorodiphenyltrichloroethane (DDT) on gene transcription and DNA methylation in the hypothalamus of young male rats: implication of hormesis-like effects. J Toxicol Sci 2009;34:469–482.
17. Giustini M, Palazzo G, Colafemmina G, Della Monica M, Giomini M, Ceglie A. Microstructure and dynamics of the water-in-oil CTAB/n-pentanol/n-hexane/water microemulsion: a spectroscopic and conductivity study. J Phys Chem 1996;100:3190–3198.
18. Caizer C, Savii C, Popovici M. Magnetic behaviour of iron oxide nanoparticles dispersed in a silica matrix. Mater Sci Eng B, 2003;97:129–134.
19. Šepelák V, Baabe D, Mienert D, Schultze D, Krumeich F, Litterst FJ, Becker KD. Evolution of structure and magnetic properties with annealing temperature in nanoscale high-energy-milled nickel ferrite. J Magn Magn Mater 2003;257:377–386.

20. Kang YS, Risbud S, Rabolt JF, Stroeve P. Synthesis and characterization of nanometer-size Fe_3O_4 and γ-Fe_2O_3 particles. Chem Mater 1996;8:2209–2211.

21. Dave SR, Gao, X. Monodisperse magnetic nanoparticles for biodetection, imaging, and drug delivery: a versatile and evolving technology. Wiley Interdiscip Rev Nanomed Nanobiotechnol 2009;1:583–609.

22. Zhang LY, Gu HC, Wang XM. Magnetite ferrofluid with high specific absorption rate for application in hyperthermia. J Magn Magn Mater 2007;311:228–233.

Figure and Table Legends

FIGURE 1. XRD patterns of samples RT-30 and RT-60, in comparison with those of starting MNPs.

FIGURE 2. SEM images of samples RT-30 and RT-60.

FIGURE 3. Size distribution curves of samples RT-30 and RT-60.

FIGURE 4. Time-dependent temperature curves of the agar phantom under a magnetic field of 100 kHz and 300 Oe.

FIGURE 5. Magnetization curves of samples measured under an applied magnetic field of 300 Oe.

FIGURE 6. DNA concentrations of Rat-1 fibroblasts cultured with different samples and with different concentrations. Data are shown as the mean ± SD (n = 5). *$P < 0.05$, **$P < 0.01$.

FIGURE 7. Representative optical micrographs of Rat-1 fibroblasts grown in medium with and without samples after 1, 3, and 7 days of culture.

TABLE 1. Saturation magnetization (*Ms*), coercive force (*Hc*), and calculated MNP contents of samples, in comparison with those of staring MNPs.

TABLE 2. Specific absorption rate (*SAR*) and heat generation calculated by the hysteresis loop (*P*) of samples.

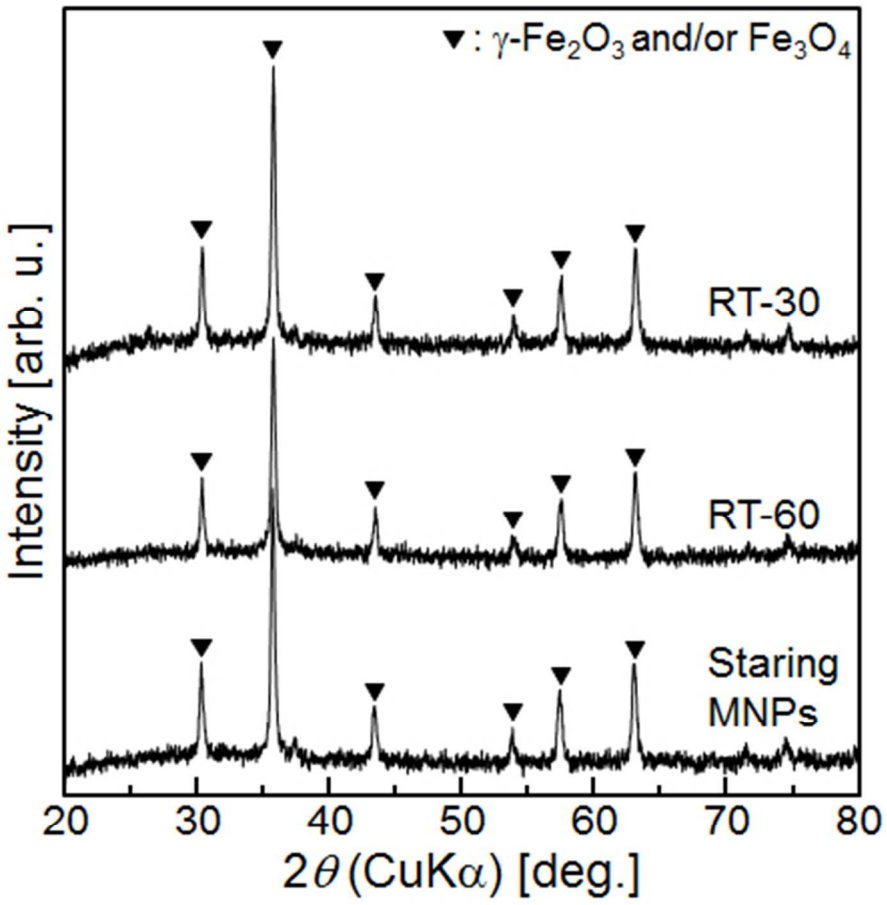

FIGURE 1. XRD patterns of samples RT-30 and RT-60, in comparison with those of starting MNPs.

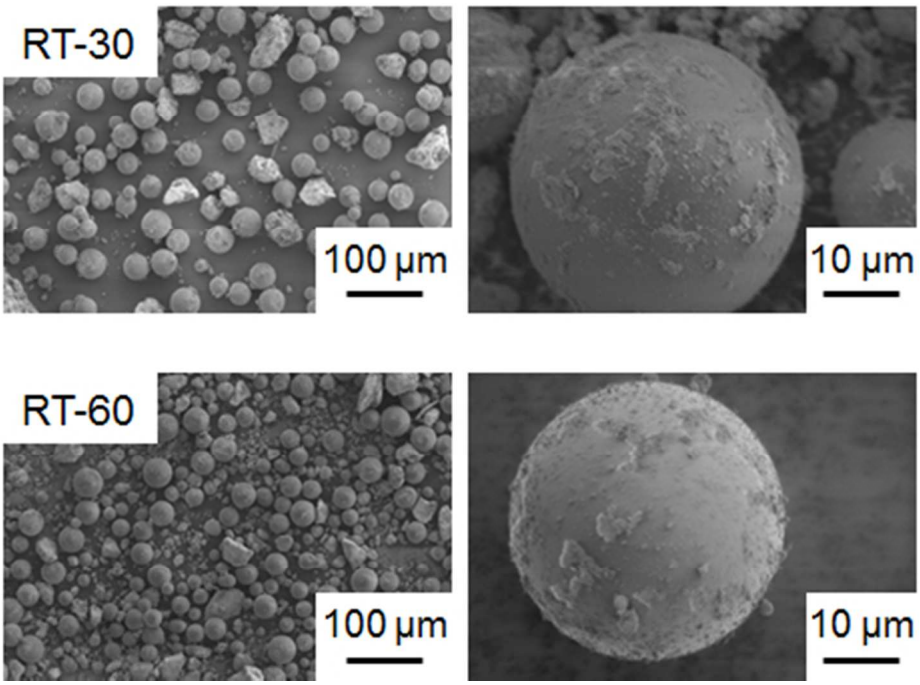

FIGURE 2. SEM images of samples RT-30 and RT-60.

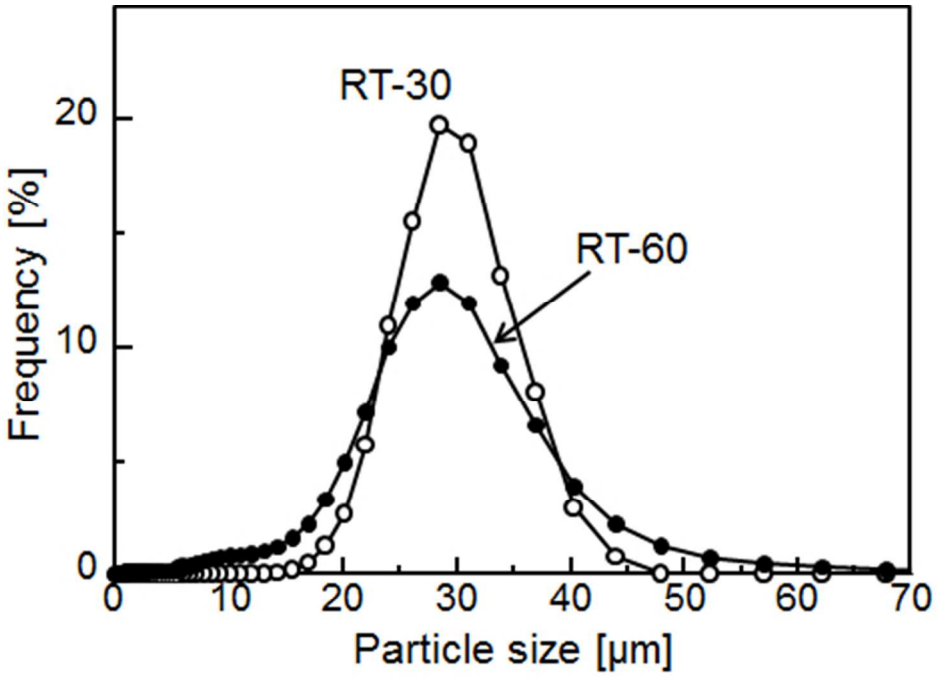

FIGURE 3. Size distribution curves of samples RT-30 and RT-60.

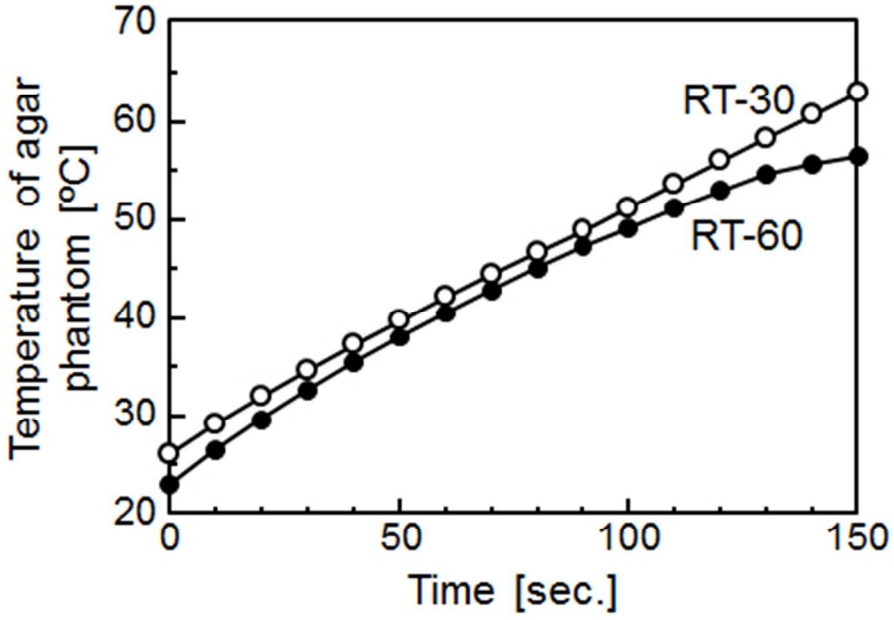

FIGURE 4. Time-dependent temperature curves of the agar phantom under a magnetic field of 100 kHz and 300 Oe.

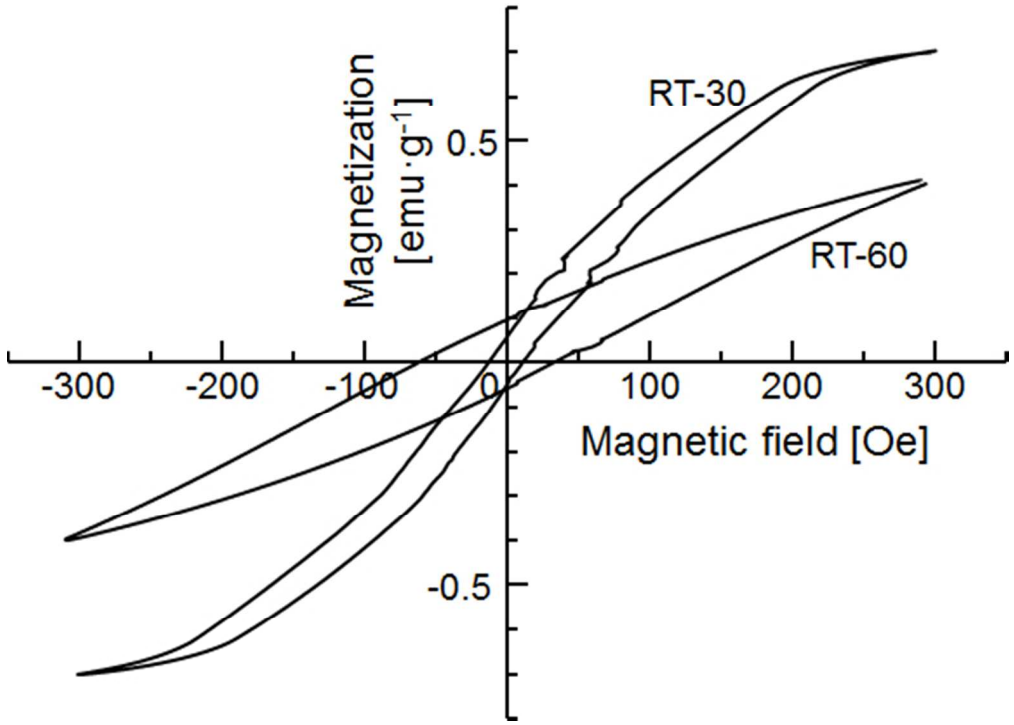

FIGURE 5. Magnetization curves of samples measured under an applied magnetic field of 300 Oe.

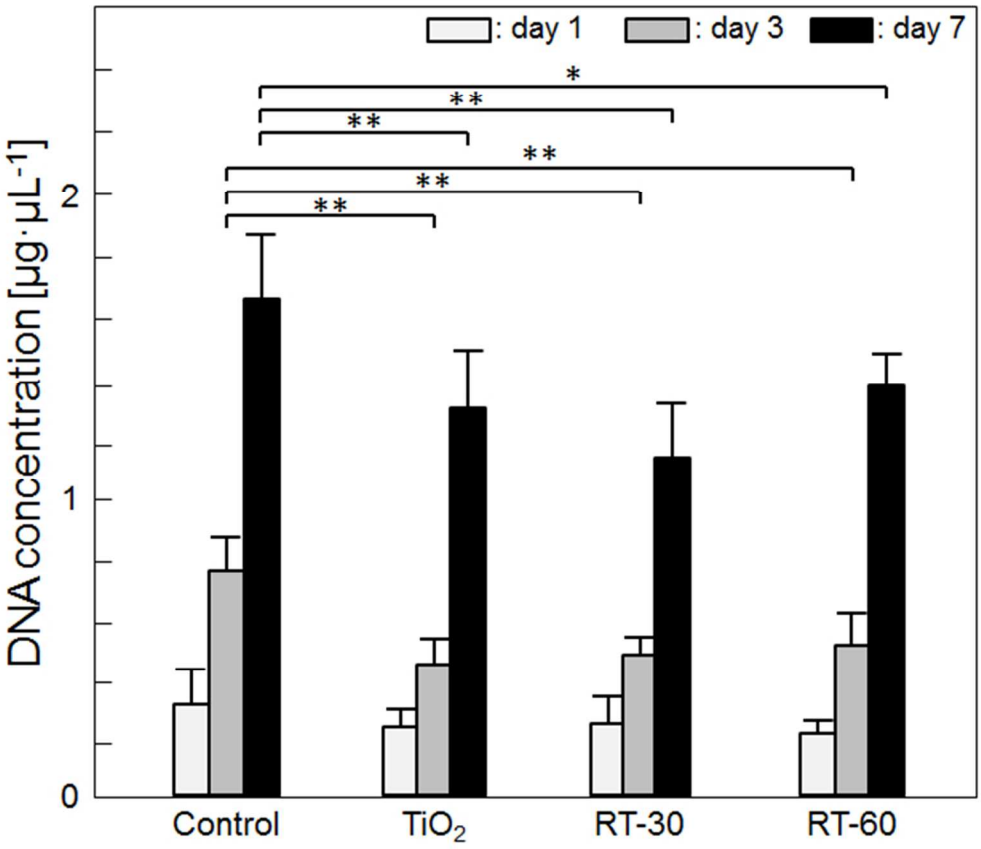

FIGURE 6. DNA concentrations of Rat-1 fibroblasts cultured with different samples and with different concentrations. Data are shown as the mean ± SD (n = 5). *$P < 0.05$, **$P < 0.01$.

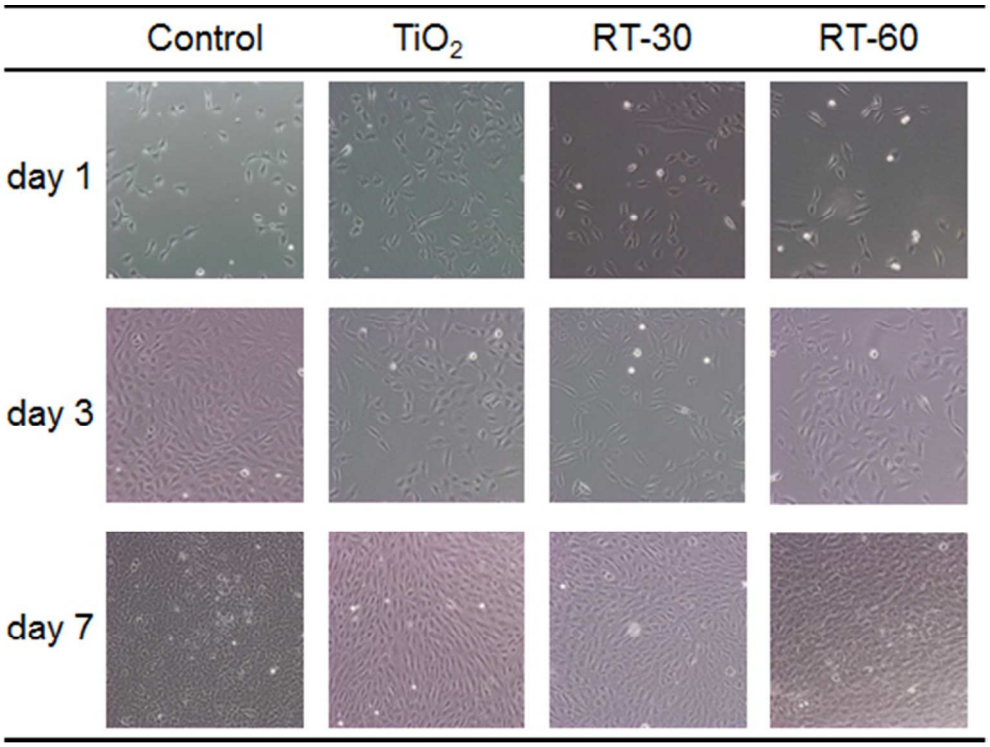

FIGURE 7. Representative optical micrographs of Rat-1 fibroblasts grown in medium with and without samples after 1, 3, and 7 days of culture.

Table 1. Saturation magnetization (*Ms*), coercive force (*Hc*) and calculated MNP contents of samples, in comparison with those of staring MNPs.

Sample	*Ms* [emu·g^{-1}]	*Hc* [Oe]	Calculated MNPs contents [wt%]
RT-30	42.8	45.0	58.5
RT-60	44.3	100	60.5
Starting MNPs	73.2	98.0	-

Table 2. Specific absorption rate (SAR) and heat generation calculated by the hysteresis loop (*P*) of samples

Sample	SAR [$W \cdot g^{-1}$]	*P* [$W \cdot g^{-1}$]
RT-30	19.2	9.1
RT-60	20.0	22.3
Starting MNPs	19.8	-